5-6

Efficient Simulation of Quantum Cascade Lasers using the Pauli Master Equation

Oskar Baumgartner, Zlatan Stanojević, and Hans Kosina
Institute for Microelectronics, TU Wien, Gußhausstraße 27–29, A–1040 Wien, Austria
Email: {baumgartner|stanojevic|kosina}@iue.tuwien.ac.at

***Abstract*—A transport model for quantum cascade lasers based on the Pauli master equation is presented. An efficient Monte Carlo solver has been developed. The numerical methods to reduce the computational cost are discussed in detail. Finally, the simulator is used to obtain current-voltage characteristics as well as microscopic quantities of a mid infrared QCL structure.**

I. Introduction

Quantum cascade lasers (QCLs) offer a wide range of advantages which make them a popular choice for coherent light sources [1]. Their light emission is based on intersubband transitions. Due to the periodic nature of QCLs a single electron will contribute repeatedly to the photon emission. The properties of the laser are mainly determined by the designer's choice of material and quantum well geometry.

For this purpose simulation is a useful tool to tune the QCL design to the desired optical and electrical characteristics. A requirement for such a simulator as design tool is a good balance between computational speed and physical accuracy. To describe the electronic properties of the laser a quantum mechanical transport model is necessary. Previously the non-equilibrium Green's function formalism (NEGF) has been used as a rigorous approach to capture the QCL's physics [2, 3]. Unfortunately the inherently high computational costs of the NEGF formalism render it unfeasible as a design tool.

II. QCL Transport Model

In our approach we use the Pauli master equation (PME) [4] to model current transport through the QCL's semiconductor heterostructure. Based on the experiences of a MATLAB prototype presented in [5], an optimized Monte Carlo (MC) simulator has been implemented in C++ within the Vienna-Schrödinger-Poisson (VSP) simulation framework [6].

A. Pauli Master Equation

Theoretical studies showed that in many practical cases the steady state transport in QCLs is incoherent and a semiclassical description was found to be sufficient [7, 8]. Following this approach, we developed a transport model for quantum cascade lasers based on the Pauli master equation [5]. The transport is described via in and out-scattering between quasi-stationary basis states, which are found by solving the Schrödinger equation. The Hamiltonian includes the band edge formed by the heterostructure, and thus, tunneling is accounted for through the delocalized eigenstates. The transport occurs via scattering between these states.

The transport equations are derived from the Liouville-von Neumann equation in the Markov limit in combination with the diagonal approximation. This means that the off-diagonal elements of the density matrix are neglected and one arrives at the Boltzmann-like Pauli master equation [9].

$$\left.\frac{\mathrm{d}}{\mathrm{d}t} f_{\mathbf{k},n}(t)\right|_{\mathrm{scat}} = \sum_{\mathbf{k}',m} \left\{ S_m^n\left(\mathbf{k}',\mathbf{k}\right) f_{\mathbf{k}',m}\left(t\right)\left[1 - f_{\mathbf{k},n}\left(t\right)\right] - S_n^m\left(\mathbf{k},\mathbf{k}'\right) f_{\mathbf{k},n}\left(t\right)\left[1 - f_{\mathbf{k}',m}\left(t\right)\right] \right\}$$

The transition rate from state $|\mathbf{k}', m\rangle$ to state $|\mathbf{k}, n\rangle$ for an interaction H_{int} follows from Fermi's golden rule

$$S_n^m\left(\mathbf{k},\mathbf{k}'\right) = \frac{2\pi}{\hbar} \left|\langle \mathbf{k}', m | H_{\mathrm{int}} | \mathbf{k}, n \rangle\right|^2 \delta\left(\mathcal{E}(\mathbf{k}') - \mathcal{E}(\mathbf{k}) \mp \hbar\omega\right).$$

We make use of the translational invariancy of the QCL structure and simulate the electron transport over a single stage only. The wave function overlap between the central stage and spatially remote stages is small. Therefore, the assumption that interstage scattering is limited only to the nearest neighbour stage holds and interactions between basis states of remote stages can be safely neglected.

The electron states corresponding to a single stage of the quantum cascade laser are determined as discussed in Sec. II-B. The states of the whole QCL device structure are assumed to be a periodic repetition of the states of a central stage. This approach ensures charge conservation and allows to impose periodic boundary conditions on the Pauli master equation.

Since transport is simulated over a central stage only, every time a carrier undergoes an interstage scattering process the electron is reinjected into the central stage with an energy changed by the voltage drop over a single period. The corresponding electron charge then contributes to the total current.

The transport equations can be solved with a Monte Carlo approach. We developed an algorithm and devised several new numerical methods to reduce the computational cost of the simulation. The implementation details will be discussed in Sec. II-C.

B. Calculation of Basis States

The task at hand can be separated into two parts. First, the basis states need to be determined. Second, the states have to be mapped to a stage according to their periodicity. For this

978-1-61284-418-3/11/$26.00 © 2011 IEEE

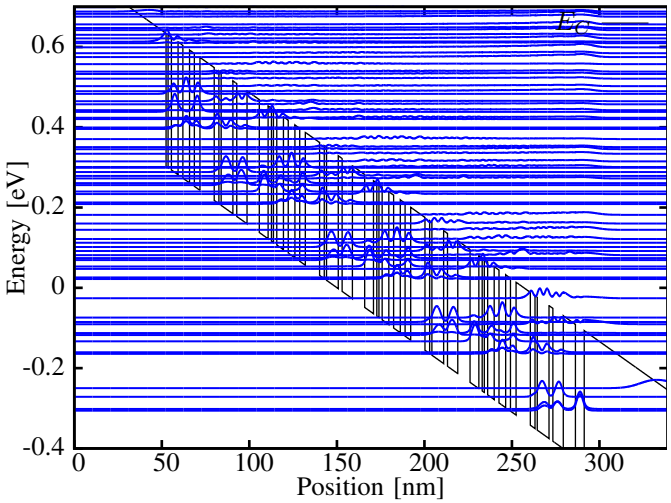

Fig. 1. Multiple cascades of a QCL need to be considered to obtain suitable basis states for the PME Monte Carlo solver.

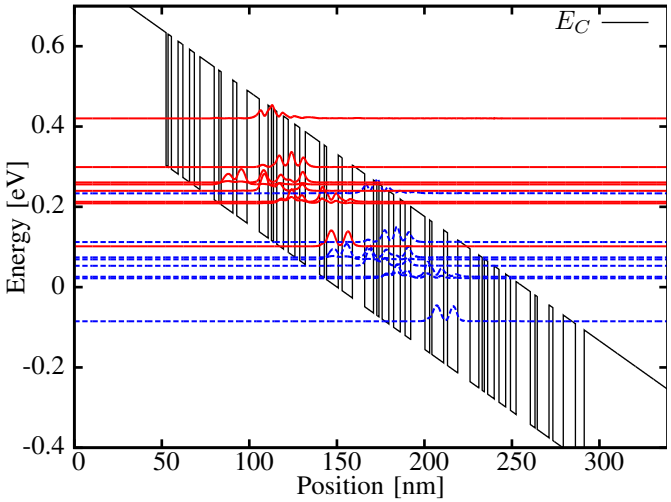

Fig. 2. Application of our subband selection routine which automatically assigns the periodic wavefunctions to a stage of the QCL (only the states of two stages are shown).

purpose the equation definition and solver facilities of the VSP were used beneficially.

Since it is essential to consider band nonparabolicity for QCLs the user can choose one of several models for the Hamiltonian of the Schrödinger equation. For this purpose, additionally to the single band effective mass model, an effective two-band $\mathbf{k}\cdot\mathbf{p}$ model [10] or a three-band $\mathbf{k}\cdot\mathbf{p}$ model are available. For the case of $\mathbf{k}_{\|} = 0$ the eight-band $\mathbf{k}\cdot\mathbf{p}$ model reduces to the three-band $\mathbf{k}\cdot\mathbf{p}$ model. Therefore, it needs not to be considered.

To describe the openness of the quantum system we make use of the perfectly matched layer (PML) boundary conditions for the Schrödinger equation [11]. Perfectly matched layers were originally used as boundary conditions for electromagnetic and waveguide problems [12]. The PML boundary conditions give rise to a general complex eigenvalue problem. It is solved by means of Arnoldi iteration and the ARPACK [13] library linked to VSP. The calculated eigenvectors correspond to the complex wavefunctions. The real part of the eigenvalue is the eigenenergy of the quasi-bound state, whereas the imaginary part can be related to its finite lifetime due to the openness of the system. This allows to estimate the tunneling current using the relation $J_{\mathrm{Tunnel}} = \sum \frac{n_i}{\tau_i}$ [14].

We calculated the eigenenergies and eigenvectors for an $In_{0.53}Ga_{0.47}As/GaAs_{0.51}Sb_{0.49}$ mid infrared (MIR) quantum cascade laser developed by [15]. The barrier thicknesses (bold) and the well thicknesses of one period in nanometer are **8.1**/2.7/**1.3**/6.7/**2.2**/5.9/**7.0**/5.0/**1.9**/1.2/**1.9**/3.8/**2.7**/3.8/**2.8**/3.2. We will use this device as benchmark throughout this paper. The calculated wavefunctions for a two-band $\mathbf{k}\cdot\mathbf{p}$ Hamiltonian with PML boundary conditions are shown in Fig. 1.

To use the eigenvectors as basis states in the MC routine we need to consider the periodicity of the device and automatically select the appropriate states of a single stage. For that purpose we calculate the cross-correlation and auto-correlation of all subbands. We make use of the relation $\mathcal{F}\{\Psi_i \star \Psi_j\} = \mathcal{F}\{\Psi_i\}^* \cdot \mathcal{F}\{\Psi_j\}$ and the Fast Fourier Transform to obtain the result quickly. Then the maxima of the correlations of all the subbands are determined. If its position equals the geometric period length of the QCL structure, the two states are considered periodic and given an appropriate stage index. As an example the periodic states of the InGaAs/GaAsSb QCL are given in Fig. 2.

C. Monte Carlo Solver

The wavefunctions provided by the routines discussed above are processed to initialize the MC code. After calculating the scattering rates using functor classes and filling the data structures, the initial valley, subband and energy of the carrier are selected randomly. In the MC loop the precalculated possible scattering processes are looked up according to the current electron state. A random number r is determined using a uniform distribution in the interval $[0, P_n]$ where $P_n = \sum_{j=1}^{n} \Gamma_j$ is the total scattering rate. The scattering process i is selected from the table such that the relation $P_{i-1} < r \leq P_i$ holds for the partial sums of the scattering rates. The data structure for the selection method is given in Fig. 3. As shown, the C++ standard template library containers are used with regard to minimize the look up time.

The current state and the chosen scattering process are used to update the statistical quantities such as subband population, energy distribution and current. Afterwards the state variable is set to its new value given by the scattering event. The MC loop is terminated, when the given number of events is reached.

To account for the periodic structure of the device the subbands of three stages are included. Whenever the electron scatters from the central to the left or right stage it is reinjected into the corresponding state of the central stage and contributes to the current.

We identified the calculation of the polar-optical phonon scattering rate as one of the major contributions to the simulation run time. Therefore, we optimized the calculation of the scattering rate for this process by exchanging the order

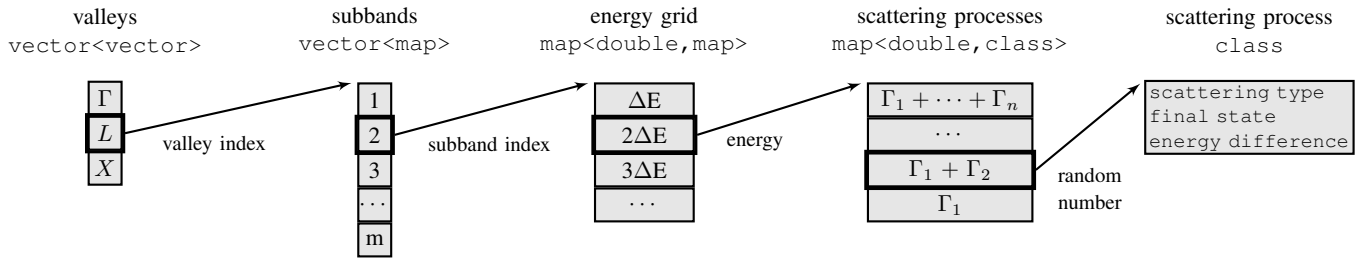

Fig. 3. Data structures for the selection of a scattering process. Valleys and subbands are accessed by index. Each subband uses its own energy grid. For a fast lookup the grid is implemented as a STL `map` with the energy as key value. Similarly, scattering processes are stored in a map where the partial sums of their transition rates are used as key. The selected scattering process instance contains all essential information to update the statistics and the state variable.

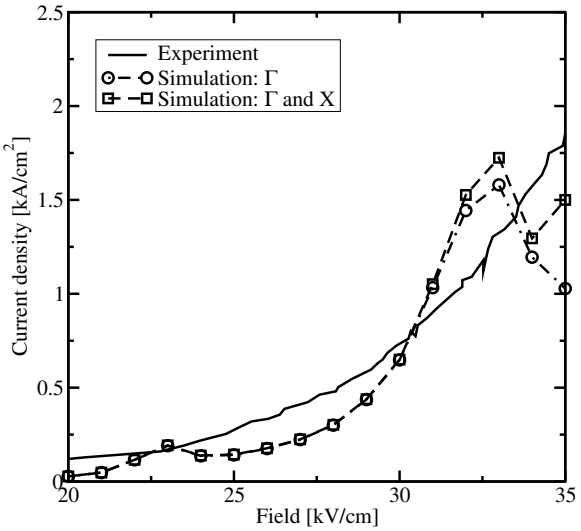

Fig. 4. Current density vs. applied electric field of the MIR QCL. The simulation shows that the inclusion of the X valley has no considerable influence on the characteristics around the laser threshold of 30kV/cm.

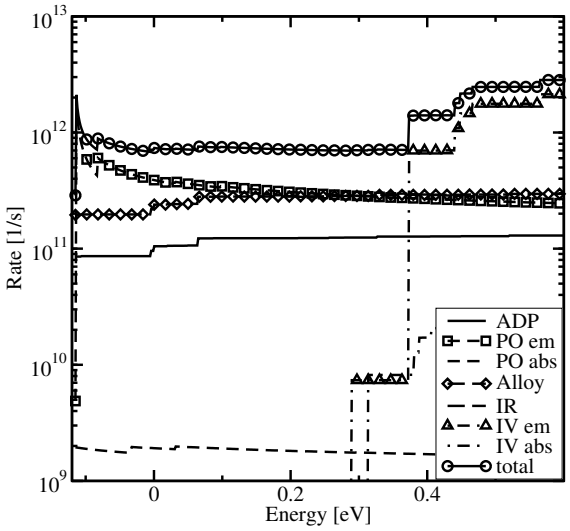

Fig. 5. Calculated scattering rates of the lower laser level. At energies near the subband minimum the polar optical emission is the dominant process. This ensures fast depopulation of the lower laser level.

of the multiple integrations. An analytic integration over the final states is carried out first. The integration related to the matrix element is carried out last. The remaining integration is in momentum space and has the form

$$\Gamma_{mn}(\mathbf{k}_\parallel) = \frac{m^*}{\hbar^2}\frac{e^2\omega_{\mathrm{PO}}}{4\pi\varepsilon}\left(n_{\mathrm{PO}}+\tfrac{1}{2}\mp\tfrac{1}{2}\right) \int \frac{|\widehat{\rho}_{mn}(q_\mathrm{z})|^2}{\sqrt{(k_\parallel^2+k_f^2+q_\mathrm{z}^2)^2-4k_\parallel^2k_f^2}}\mathrm{d}q_\mathrm{z}$$

where $k_f^2 = k_\parallel^2 + \frac{2m^*}{\hbar^2}\left(\mathcal{E}_m - \mathcal{E}_n \pm \hbar\omega_{\mathrm{PO}}\right)$ has to be positive to satisfy energy conservation. This allows us to use a Fast Fourier Transform (FFT) to exactly calculate the overlap integrals $\widehat{\rho}_{mn}(q_\mathrm{z}) = \mathcal{F}\{\rho_{mn}(z)\}$ where $\rho_{mn}(z) = \psi_m^*(z)\psi_n(z)$ which reduces the calculation time of the PO scattering rate by three to four orders of magnitude.

Currently, acoustic and optical deformation potential, and polar optical electron-phonon scattering as well as alloy, intervalley and interface roughness scattering are included. The object oriented implementation allows for simple inclusion of additional physics for further investigation of QCL devices such as electron-electron and electron-photon interaction.

III. Results and Discussion

We used the implemented transport model to simulate the InGaAs/GaAsSb mid infrared (MIR) quantum cascade laser from [15]. The electric field vs. current density characteristics at 78 Kelvin are shown in Fig. 4. The simulation result is in good agreement with the experiment. The current peak around the laser threshold can be attributed to a PO phonon resonance in the laser design for fast depletion of the lower laser level. The current drop above threshold is due to increasing coherent tunneling to the continuum as well as the electron-photon interaction not yet included in the model. The characteristics show that transport in the X valley contributes only marginally to the total current near the laser threshold. This is also indicated by the scattering rates for the lower laser level (Fig. 5) where PO emission is also shown to be dominant.

The calculation of a single operating point typically takes a few minutes, depending on number of valleys, subbands and energy grid resolution. This is orders of magnitude faster than a full quantum treatment using non-equilibrium Green's functions, but still gives insight to microscopic quantities such as the carrier density spectrum shown in Fig. 6.

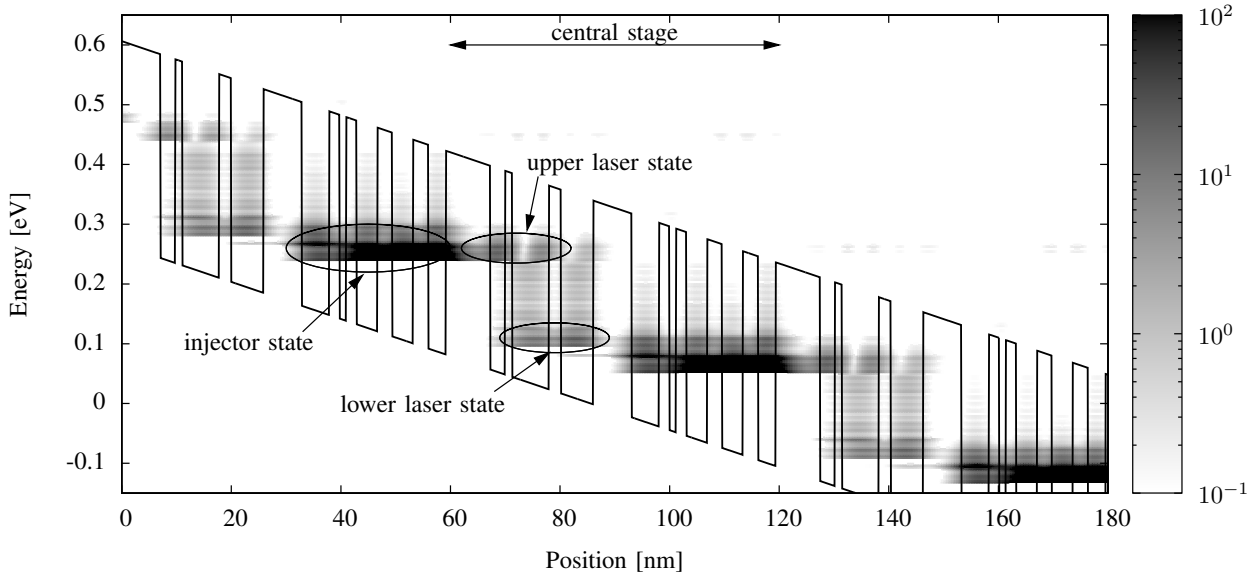

Fig. 6. Conduction band edge and carrier density spectrum obtained by the Pauli master equation solver at an electric field strength of 30kV/cm. The occupation of the upper laser state is clearly visible.

IV. Conclusion

We have presented a semiclassical transport model for quantum cascade lasers based on the Pauli master equation. We devised new numerical methods to reduce the computational demand and realized an efficient Monte Carlo simulator implemented in C++. The model was applied to a mid infrared QCL. It gives insight to macroscopic and microscopic quantities such as current-voltage characteristics, scattering rates, carrier density spectrum, subband population, and optical gain.

Acknowledgment

This work was supported by the Austrian Science Fund special research program IR-ON (F2509).

References

[1] C. Gmachl *et al.*, "Recent progress in quantum cascade lasers and applications," *Rep. Progr. Phys.*, vol. 64, no. 11, pp. 1533–1601, 2001.

[2] T. Kubis and P. Vogl, "Self-consistent quantum transport theory: Applications and assessment of approximate models," *J. Comput. Electron.*, vol. 6, pp. 183–186, 2007.

[3] S. C. Lee and A. Wacker, "Quantum transport calculations for quantum cascade laser structures," *Physica E*, vol. 13, no. 2-4, pp. 858–861, March 2002.

[4] M. V. Fischetti, "Master-equation approach to the study of electronic transport in small semiconductor devices," *Phys. Rev. B*, vol. 59, no. 7, pp. 4901–4917, February 1999.

[5] G. Milovanovic and H. Kosina, "A semiclassical transport model for quantum cascade lasers based on the Pauli master equation," *J. Comput. Electron.*, vol. 9, pp. 211–217, 2010.

[6] M. Karner *et al.*, "A Multi-Purpose Schrödinger-Poisson Solver for TCAD Applications," *J. Comput. Electron.*, vol. 6, no. 1, pp. 179–182, September 2007.

[7] R. C. Iotti and F. Rossi, "Nature of Charge Transport in Quantum-Cascade Lasers," *Phys. Rev. Lett.*, vol. 87, no. 14, p. 146603, September 2001.

[8] C. Jirauschek *et al.*, "Comparative analysis of resonant phonon THz quantum cascade lasers," *J. Appl. Phys.*, vol. 101, no. 8, p. 086109, 2007.

[9] R. C. Iotti *et al.*, "Quantum transport theory for semiconductor nanostructures: A density-matrix formulation," *Phys. Rev. B*, vol. 72, no. 12, p. 125347, Sep 2005.

[10] C. Sirtori *et al.*, "Nonparabolicity and a sum rule associated with bound-to-bound and bound-to-continuum intersubband transitions in quantum wells," *Phys. Rev. B*, vol. 50, no. 12, pp. 8663–, September 1994.

[11] S. Odermatt *et al.*, "Bandstructure calculation using the $\mathbf{k}\cdot\mathbf{p}$ method for arbitrary potentials with open boundary conditions," *J. Appl. Phys.*, vol. 97, no. 4, p. 046104, 2005.

[12] J.-P. Berenger, "A perfectly matched layer for the absorption of electromagnetic waves," *J. Comput. Phys.*, vol. 114, no. 2, pp. 185 – 200, 1994.

[13] R. B. Lehoucq *et al.*, *ARPACK Users' Guide: Solution of Large-Scale Eigenvalue Problems with Implicitly Restarted Arnoldi Methods*. SIAM, 1998.

[14] R. Clerc *et al.*, "Theory of direct tunneling current in metal–oxide–semiconductor structures," *J. Appl. Phys.*, vol. 91, no. 3, pp. 1400–1409, February 2002.

[15] M. Nobile *et al.*, "Quantum cascade laser utilising aluminium-free material system: InGaAs/GaAsSb lattice-matched to InP," *Electron. Lett*, vol. 45, no. 20, pp. 1031 –1033, 24 2009.